Available online at www.sciencedirect.com

ScienceDirect

IFAC PapersOnLine 55-41 (2022) 32–37

Light Guidance Control of Human Drivers: Driver Modeling, Control System Design, and VR Experiment

M. Takeda * **M. Inoue** * **X. Fang** * **Y. Minami** ** **J. M. Maestre** ***

* *Keio University, Yokohama, Japan (e-mail: masahiko0322@keio.jp, minoue@appi.keio.ac.jp)*

** *Osaka University, Suita, Japan (e-mail: minami@mech.eng.osaka-u.ac.jp)*

*** *University of Seville, Seville, Spain (e-mail: pepemaestre@us.es)*

Abstract: This paper addresses light guidance control for human-driven vehicles. We manipulate pace-making-light (PML) installed in the road environment to make drivers accelerate their vehicles unconsciously. Also, since the performance of the control system relies on the human reaction, we address the modeling of the driver's behavior guided by PML. To this end, we tested human subjects by using a driving simulator developed in a virtual reality environment. The collected data were used to model the driver's behavior and to perform a PML control simulation. In particular, the driver model is utilized for the design of a model predictive controller that is implemented as the PML logic.

Keywords: Light guidance control, Human-in-the-loop, Driver modeling, Virtual reality experiment

1. INTRODUCTION

Frequent traffic congestions cause significant economic losses, air pollution, and an increase in traffic accidents. As studied by Koshi and Kuwaham (1992), one of the main causes of traffic congestion on highways is unconscious deceleration by drivers at the entrance of tunnels. For this reason, control technology needs to be further developed and applied to prevent unconscious deceleration.

The most effective approach to preventing unconscious deceleration is controlling autonomous vehicles (AVs). Assuming that all vehicles are fully automated and allow the intervention of the infrastructure side, unconscious deceleration can be avoided. However, as reported by Alessandrini et al. (2015), the penetration of AVs will not reach 100 percent before 2060.

For the decades to come, human-driven vehicles (HDVs) need to be taken into account in addition to AVs. As pointed out by, e.g., Wang et al. (2021), Feng et al. (2021), and Liu et al. (2022), a mixed traffic control, focused on the interactions between AVs and HDVs, needs to be addressed. In most of the related references, control systems typically actuate AVs so that the overall vehicle platoon is stabilized and traffic flow improves despite the disturbances caused by HDVs. An exceptional work presented by Kari et al. (2021) considers the actuation of human drivers in HDVs by using scene-adaptive music to give awareness to drivers on some upcoming events such as the entrance of a tunnel. Such "indirect" control of HDVs, i.e., without compulsory actions for the drivers, is based on the unconscious behavior of drivers.

Inspired by the indirect control approach proposed by Kari et al. (2021), this paper explores another indirect control mechanism of HDVs by using pace-making-light (PML). PML consists of multiple lights and is installed in tunnels on highways as shown in Fig. 1. Moving lights can induce drivers to accelerate their vehicles based on their unconscious reactions. The work by Watanabe et al. (2018) investigated the effect of the light guidance control and showed its potential to mitigate traffic congestion. To further improve the performance of the light guidance control, which relies on human unconscious reaction, we propose to model the driver's reaction and employ a model-based approach for the control logic that needs to be designed.

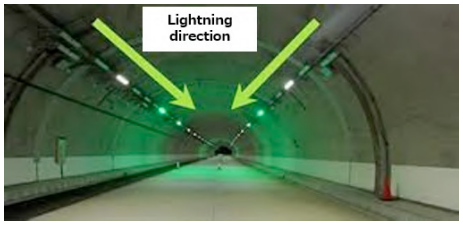

Fig. 1. PML installed in Shinmeishin highway (National Secretariat Technical Research Division (2021)).

This paper is devoted to the design of a light guidance control system composed of HDVs and PML. To this end, the modeling of the driver and the design of a model-based controller are addressed. The driver's behavior is modeled by a multi-loop structure composed of manual and unconscious control parts. Then, model predictive control (MPC) is employed so that frequent changes in the PML velocity are avoided, which results in drivers following the PML lighting without getting any discomfort. The contributions of this paper are as follows: 1) we propose a structure for the driver model in the presence of PML; 2) we propose a "human-centered" control logic for the PML so that drivers do not get any discomfort; 3) we test and assess the reactions of human subjects using a driving simulator developed in a virtual reality (VR) environment.

⋆ This work is supported by Grant-in-Aid for Scientific Research (B), No. 20H04473 from JSPS.

⋆⋆Financial support from MCIN/AEI/10.13039/501100011033 project C3PO-R2D2 under grant PID2020-119476RB-I00 is gratefully acknowledged.

10.1016/j.ifacol.2023.01.099

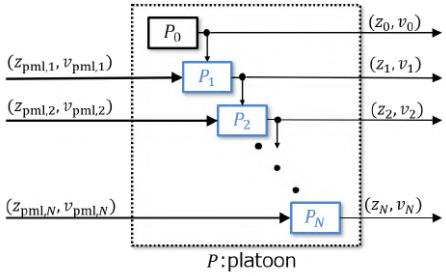

Fig. 2. Block diagram of the HDVs in the platoon,

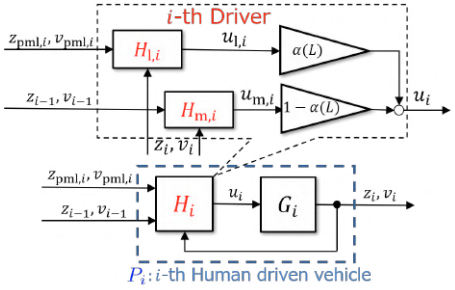

Fig. 3. Block diagram of the i-th HDV.

The remainder of the paper is organized as follows. In Section 2, we model HDVs that include human unconscious reactions to PML lighting. In Section 3, we present the control law implemented in the PML. In Section 4, we perform VR experiments to collect data on driver behavior and obtain the corresponding model. Then, we perform simulations to validate the present control system.

2. PLANT MODELING

In this section, we model a group of HDVs guided by PML. In a situation with high traffic density, the group automatically constitutes a vehicle platoon. Let the leading HDV in the platoon be denoted by P_0, and the following N HDVs be denoted by P_i, $i \in \{1, \cdots, N\}$. In particular, we consider that the second HDV, denoted by P_1, decelerates at the entrance of a tunnel and is to be guided by the PML.

The structure of the HDVs in the platoon is illustrated in Fig. 2. In the figure, (z_i, v_i) represents the position and the velocity of P_i and $(z_{\mathrm{pml},i}, v_{\mathrm{pml},i})$ represents those of the PML that targets P_i. Each P_i, $i \in \{1, \cdots, N\}$, is assumed to behave as a feedback control system composed of vehicle dynamics and driver behavior, see Fig. 3. In the figure, G_i and H_i represent the vehicle and the driver of P_i, respectively. Furthermore, each driver H_i is modeled by a multi-loop controller. One loop models the manual control, denoted by $H_{\mathrm{m},i}$, used to regulate the vehicle state based on the state of P_{i-1}. The second loop models the unconscious control, denoted by $H_{\mathrm{l},i}$, to intervene in the driver's control action based on the state of the PML. Note that the unconscious control $H_{\mathrm{l},i}$ works only when PML is visible to the driver. The details of G_i, $H_{\mathrm{m},i}$, and $H_{\mathrm{l},i}$ are given as below.

2.1 Vehicle dynamics

As in the work by Rajamani (2011), the longitudinal dynamics of the i-th vehicle G_i are modeled by the first-order system

$$G_i : \ a_i(k+1) = \frac{(T_i - \Delta t)a_i(k) + K_i \Delta t u_i(k)}{T_i}, \quad (1)$$

where k is the discrete time index, Δt is the sampling period, $a_i(k)$ is the acceleration of P_i, $u_i(k)$ is the action performed on the accelerator of P_i, and K_i and T_i are the gain and the time constant, respectively.

2.2 Driver dynamics

The driver's behavior H_i is determined by the combination of $H_{\mathrm{m},i}$ and $H_{\mathrm{l},i}$. Let $u_{\mathrm{m},i}$ and $u_{\mathrm{l},i}$ be the outputs of $H_{\mathrm{m},i}$ and $H_{\mathrm{l},i}$, respectively, $\alpha_i(L)$ be the percentage of the driver's awareness that is allocated to the PML, and L be the binary variable that represents the status of PML, i.e., $L = 1$ means that PML is working, while $L = 0$ means that PML is not working. Then, the driver's action $u_i(k)$ on the accelerator is described by

$$H_i : u_i(k) = (1 - \alpha_i(L))u_{\mathrm{m},i}(k) + \alpha_i(L)u_{\mathrm{l},i}(k), \quad (2)$$

where $\alpha_i(L)$, $L \in \{0, 1\}$ satisfies $\alpha_i(0) = 0$ and $\alpha_i(1) \in (0, 1]$.

The models of $H_{\mathrm{m},i}$ and $H_{\mathrm{l},i}$ are given as follows:

- Manual control part $H_{\mathrm{m},i}$
  The driver of the HDV P_i aims at keeping a desired distance to the HDV P_{i-1} based on the measurement of the distance and the relative velocity. Let $\delta_{\mathrm{m},i}$ be the desired distance between the HDVs P_i and P_{i-1}, which includes the length of the HDV P_{i-1}. Then, the manual control model can be described as
  $$H_{\mathrm{m},i} : \ u_{\mathrm{m},i}(k) = K_{\mathrm{m},i}(z_{i-1}(k) - z_i(k) - \delta_{\mathrm{m},i}) + C_{\mathrm{m},i}(v_{i-1}(k) - v_i(k)), \quad (3)$$
  where $K_{\mathrm{m},i}$ and $C_{\mathrm{m},i}$ are constants.
- Unconscious control part $H_{\mathrm{l},i}$
  Drivers may tend to follow the position of the PML, due to unconscious response to light guidance, as studied by Kawashima et al. (2012). Let $\delta_{\mathrm{l},i}$ be the desired distance between the HDV P_i and the PML. Then, the unconscious control model can be described as
  $$H_{\mathrm{l},i} : \ u_{\mathrm{l},i}(k) = K_{\mathrm{l},i}(z_{\mathrm{pml},i}(k) - z_i(k) - \delta_{\mathrm{l},i}) + C_{\mathrm{l},i}(v_{\mathrm{pml},i}(k) - v_i(k)), \quad (4)$$
  where $K_{\mathrm{l},i}$ and $C_{\mathrm{l},i}$ are constants.

The overall dynamics of P_i are described by the following state-space equation. Let

$$x_i(k) = [z_i(k) \ v_i(k) \ a_i(k)]^\top,$$
$$u_{\mathrm{pml},i}(k) = [z_{\mathrm{pml},i}(k) \ v_{\mathrm{pml},i}(k)]^\top,$$
$$\delta_i = [\delta_{\mathrm{m},i} \ \delta_{\mathrm{l},i}]^\top.$$

Then, the equations given in (1)-(4) are reduced to the state equation

$$x_i(k+1) = A_i(L)x_i(k) + B_{x,i}(L)x_{i-1}(k) + B_{\mathrm{l},i}(L)u_{\mathrm{pml},i}(k) + D_i(L)\delta_i, \quad (5)$$

where $A_i(L)$, $B_{x,i}$, $B_{\mathrm{l},i}(L)$ and D_i are the system matrices. (Details are omitted due to the limitation of pages.)

3. CONTROL SYSTEM DESIGN

The control system composed of platoon P, controller $\mathcal{K}$, and supervisor $\mathcal{S}$ is shown in Fig. 4. In the figure, supervisor $\mathcal{S}$ observes the velocity of all the HDVs, denoted by $\{v_i\}$, to determine the control target. Symbol $\mathcal{I}_{\mathrm{tar}}$ denotes the set of

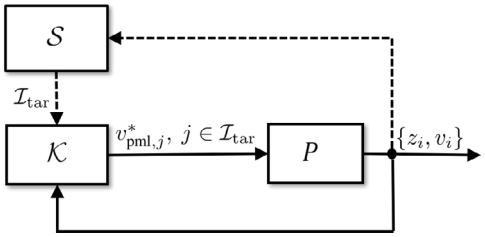

Fig. 4. Overall control system.

labels of target HDVs, which satisfies $\mathcal{I}_{\rm tar} \subseteq \{1,\dots,N\}$. Controller $\mathcal{K}$ utilizes the state of all HDVs, denoted by $\{z_i, v_i\}$ to determine the PML velocity, denoted by $v^*_{{\rm pml},j},\ j \in \mathcal{I}_{\rm tar}$. The control cycle for controller $\mathcal{K}$ is Δt, while that for supervisor S is $\Delta t_{\rm s}$, satisfying $\Delta t < \Delta t_{\rm s}$. Then, each vehicle P_i is driven by the combination of manual control $H_{{\rm m},i}$ and unconscious control $H_{{\rm l},i}$ to generate (z_i, v_i).

The following two subsections are devoted to the design of the supervisor $\mathcal{S}$ and controller $\mathcal{K}$.

3.1 Supervisor

We present an algorithm applied in supervisor $\mathcal{S}$, which determines the control target.

Let $e_i(k)$ be the relative velocity between P_0 and P_i, i.e.,

$$v_{{\rm e},i}(k) = v_0(k) - v_i(k).$$

Recalling that driver 1 decelerates at the entrance of the tunnel, it naturally holds that $1 \in \mathcal{I}_{\rm tar}$. Furthermore, the other targets are determined based on the absolute value of $v_{{\rm e},i}$, $i \in \{2,\cdots,N\}$, by applying the following algorithm.

The mechanism employed for the target selection is detailed in Algorithm 1.

Algorithm 1 Target selection

```
Measure {v_i(k)}
The target set is initialized as I_tar = {1}.
for i = 2 : N :
    if v_{e,i}(k) ≥ γ_on :
        The target set is updated as I_tar ← I_tar ∪ {i}.
    end
    if v_{e,i}(k) ≤ γ_off and i ∈ I_tar :
        The target set is updated as I_tar ← I_tar \ {i}.
    end
end
```

Note that in the algorithm $\gamma_{\rm on}$ and $\gamma_{\rm off}$ are constants satisfying $\gamma_{\rm on} > \gamma_{\rm off}$, which are determined that chattering on PML lighting is avoided. Assuming that P_j is the control target, i.e., $j \in \mathcal{I}_{\rm tar}$, PML starts lighting at $(z_{{\rm pml},j}, v_{{\rm pml},j}) = (z_j + \delta_{{\rm l},j}, v_0)$.

3.2 Controller

We address the design of the controller $\mathcal{K}$ to be implemented in the PML.

Let j be the label of a control target, i.e., $j \in \mathcal{I}_{\rm tar}$ and $\star(\tau|k)$ be the predicted value of $\star$ at τ steps ahead from the current time k. Then, the series of the predicted velocities of P_j and PML is stacked as

$$\boldsymbol{V}_j = [v_j(0|k)\ \cdots\ v_j(H|k)] \in \mathbb{R}^{H+1},$$

$$\boldsymbol{V}_{{\rm pml},j} = [v_{{\rm pml},j}(-1|k)\ \cdots\ v_{{\rm pml},j}(H-1|k)] \in \mathbb{R}^{H+1},$$

respectively.

Then, let J be the objective function, J is expressed in vector form as

$$J = \|\boldsymbol{V}_{j-1} - \boldsymbol{V}_j\|_{2,Q} + \|\Psi \boldsymbol{V}_{{\rm pml},j}\|_{1,R}. \tag{6}$$

where $\|\cdot\|_{2,Q}$ is the weighted L_2 norm, $\|\cdot\|_{1,R}$ is the weighted L_1 norm, and $Q \in \mathbb{R}^{(H+1)\times(H+1)}$, $R \in \mathbb{R}^{H\times H}$ and $\Psi \in \mathbb{R}^{H\times(H+1)}$ are constant matrices given by

$$Q = Q_1 + Q_2,$$
$$Q_1 = {\rm diag}([q_1,\cdots,q_{H+1}]),$$
$$Q_2 = \begin{bmatrix} H+1 & H & \cdots & 1 \\ H & H & \cdots & 1 \\ \vdots & \ddots & \ddots & \vdots \\ 1 & \cdots & 1 & 1 \end{bmatrix},$$
$$R = {\rm diag}([r_1,\cdots,r_H]),$$
$$\Psi = \begin{bmatrix} -1 & 1 & & \mathcal{O} \\ & -1 & 1 & \\ & & \ddots & \ddots \\ \mathcal{O} & & & -1\ \ 1 \end{bmatrix}.$$

In (6), the first term contributes to preventing disturbance propagation to the following vehicles, while the second term contributes to avoiding frequent changes in the PML velocity.

Recall that controller $\mathcal{K}$ is driven by the measured states of P_j and P_{j-1}, denoted by $x_j(k)$ and $x_{j-1}(k)$, respectively. In controller $\mathcal{K}$, an optimization problem is solved on every control cycle Δt. We suppose that the PML velocity is given by $v_{{\rm pml},j}(k-1)$ at control cycle $k-1$. Also, we initialize the prediction of the state as $v_{{\rm pml},j}(-1|k) = v_{{\rm pml},j}(k-1)$, $z_{{\rm pml},j}(0|k) = z_{{\rm pml},j}(k)$, $x_j(0|k) = x_j(k)$ and $z_{j-1}(0|k) = z_{j-1}(k)$. Then, the following optimization problem is addressed in controller $\mathcal{K}$:

$$\min_{\boldsymbol{V}_{{\rm pml},j}} \ J \tag{7a}$$

subject to

$$x_j(\tau+1|k) = A_j(L)x_j(\tau|k) + B_{x,j}(L)x_{j-1}(\tau|k) + B_{{\rm l},j}(L)u_{{\rm pml},j}(\tau|k) + D_j(L)\delta_j, \tag{7b}$$
$$v_{j-1}(\tau|k) = v_{j-1}(k), \tag{7c}$$
$$z_{j-1}(\tau+1|k) = z_{j-1}(\tau|k) + \Delta t v_{j-1}(\tau|k), \tag{7d}$$
$$z_{{\rm pml},j}(\tau+1|k) = z_{{\rm pml},j}(\tau|k) + \Delta t v_{{\rm pml},j}(\tau|k), \tag{7e}$$
$$v_{\rm min} \le v_{{\rm pml},j}(\tau|k) \le v_{\rm max}, \tag{7f}$$
$$|v_{{\rm pml},j}(\tau|k) - v_{{\rm pml},j}(\tau-1|k)| \le v_{\rm ch}, \quad \forall \tau \in \{0,\dots,H-1\}. \tag{7g}$$

Let $\boldsymbol{V}^*_{{\rm pml},j}$ be the solution of the optimization problem (7). In controller $\mathcal{K}$, the PML velocity, $v_{{\rm pml},j}(k)$, is determined by the second element of $\boldsymbol{V}^*_{{\rm pml},j}$. The goals of imposing the constraints are as follows: constraint (7b) is the model-based state prediction of P_j; (7c) and (7d) are the state prediction of P_{j-1}; (7e) is the position prediction of PML; (7f) bound the PML velocity; (7g) bound the change of the PML velocity. In particular, (7g) is introduced so that the drivers do not get any discomfort.

4. VR EXPERIMENT AND CONTROL SIMULATION

4.1 Data-driven Driver Modeling with VR Experiment

One of the main problems in driver modeling is the high cost of conducting experiments using actual vehicles. A solution is

Fig. 5. Driving simulator.

to use simulation games to collect driver data as performed by Ozkan et al. (2021) and Hara et al. (2021). In this paper, we test human subjects using a driving simulator. Then, the collected data on human driving behavior is utilized for parameter estimation in (2)-(4).

The driving simulator utilized is shown in Fig. 5. The simulator has been developed with Unity and designed for use in a VR environment. The interface to the VR environment is Oculus Quest 2. The acceleration and deceleration commands of the human subject, using the driving simulator, are conducted by the right-hand and left-hand controllers, respectively.

In this subsection, P_1 is the vehicle operated by the human subject and P_0 is the preceding vehicle operated by a simple control logic stated in the experiment procedure below. Every sampling period Δt, the data on the acceleration and the velocity of the target vehicle, the preceding vehicle, and the PML, denoted by $u_1(k), v_1(k), v_0(k)$ and $v_{\text{pml},1}(k)$, respectively, are collected. In the following discussion, details on the experiment setups and modeling results are given.

Procedure for VR Experiment At the beginning of each experiment $k = 0$, the state of P_1 is set as $(z(0), v(0)) = (0, 0)$. Let k_{up} and k_{on} represent the time instant after v_1 is kept in $[77,\ 83]$ km/h for 5 seconds and z_1 reaches 1000, respectively. In addition, k_{end} denotes the termination time. The human subject performs the VR tests using the following procedure:

Stage I: Experiment 1 to Model Manual Control

The goal of this stage is to collect data for parameter identification of manual control $H_{\text{m},1}$. Each subject performs the same experiment repeatedly for fifteen times under the following setup: P_0 behaves as

$$z_0(0) = 10,\ v_0(k) = \begin{cases} 2\Delta t k, & k \in [\,0,\ 35/\Delta t\,] \\ 70, & k \in [\,35/\Delta t,\ k_{\text{up}}\,] \\ 80, & k \in [\,k_{\text{up}},\ k_{\text{end}}\,]. \end{cases}$$

In this experiment, PML is not turned on.

Stage II: Experiment 2 to Model Unconscious Control

The goal of this stage is to collect data for parameter identification of unconscious control $H_{\text{l},1}$. Each subject performs the same experiment repeatedly for fifteen times under the following setup: no preceding vehicle exists, but PML is turned on and behaves as

$$z_{\text{pml},1}(0) = 0,\ v_{\text{pml},1}(k) = \begin{cases} 2\Delta t k, & k \in [\,0,\ 35/\Delta t\,] \\ 70, & k \in [\,35/\Delta t,\ k_{\text{up}}\,] \\ 80, & k \in [\,k_{\text{up}},\ k_{\text{end}}\,]. \end{cases}$$

Stage III: Experiment 3 to Model Overall Driver Behavior

The goal of this stage is to collect data for parameter identification of the driver's behavior H_1. Each subject performs the same experiment repeatedly for fifteen times under the following setup: P_0 behaves as

$$z_0(0) = 10,\ v_0(k) = \begin{cases} 2\Delta t k, & k \in [\,0,\ 40/\Delta t\,] \\ 80, & k \in [\,40/\Delta t,\ k_{\text{end}}\,], \end{cases}$$

and the PML is turned on and behaves as

$$z_{\text{pml},1}(0) = 1020,\ v_{\text{pml},1}(k) = \begin{cases} 0, & k \in [\,0,\ k_{\text{on}}\,] \\ 80, & k \in [\,k_{\text{on}},\ k_{\text{end}}\,]. \end{cases}$$

Table 1. Average RMSE of driver model

Stage I	Stage II	Stage III
1.56	2.61	1.01

Result of the Driver Modeling In the system identification, only the data of $k_{\text{up}} \le k \le k_{\text{end}}$, which corresponds to Stages I and II, and that of $k_{\text{on}} \le k \le k_{\text{end}}$, which corresponds to Stage III, are extracted. The data collected in the fifteen trials are divided into two datasets: the data for the first ten trials is used for training, while that for the last five trials is used for validation. The identification procedure is stated as follows:

(I) The least-squares method is applied for each training data to obtain ten sets of model parameters in $(K_{\text{m},1}, C_{\text{m},1}, K_{\text{l},1}, C_{\text{l},1})$. In addition, the data on the distance in HDV and PML during $k_{\text{end}} - 2/\Delta t \le k \le k_{\text{end}}$ is used to estimate $(\delta_{\text{m},1}, \delta_{\text{l},1},\ \alpha_1(1))$.

(II) The average value of $(K_{\text{m},1}, C_{\text{m},1}, \delta_{\text{m},1}, K_{\text{l},1}, C_{\text{l},1}, \delta_{\text{l},1}, \alpha_1(1))$ is calculated to determine the model parameters in (2)-(4).

(III) The model accuracy is evaluated using the validation data as the average value of the root mean square error (average RMSE):

$$\sum_{p=1}^{5} \frac{1}{5} \sqrt{\frac{1}{n} \sum_{k=0}^{n-1} (v(k) - v_{\text{val},p}(k))^2},$$

where $v_{\text{val},p},\ p \in \{1, \cdots, 5\}$, is the velocity of each validation data set.

Following this procedure conducted on one person who know what was going to be modeled, we obtained the following driver model:

$$\begin{aligned} H_{\text{m},i}:\ u_{\text{m},i}(k) = {} & 0.135(z_{i-1}(k) - z_i(k) - 20.6) \\ & + 0.142(v_{i-1}(k) - v_i(k)), \end{aligned} \tag{8}$$

$$\begin{aligned} H_{\text{l},i}:\ u_{\text{l},i}(k) = {} & 0.162(z_{\text{pml},i}(k) - z_i(k) - 13.8) \\ & + 0.100(v_{\text{pml},i}(k) - v_i(k)), \end{aligned} \tag{9}$$

$$H: u_i(k) = 0.524 u_{\text{m},i}(k) + 0.476 u_{\text{l},i}(k). \tag{10}$$

The constructed model is compared with the validation data collected in Stages I-III in Fig. 6. In the figure, the black lines represent the model outputs and the blue regions represent the mean $\pm$ standard deviation of the validation data. We see that the model expresses the averaged behavior in the validation data and the HDV behavior fluctuates largely in the case of sole PML control as shown in Fig. 6(b), while it is suppressed when the preceding HDV exists as shown in Figs. 6(a) and 6(c). This implies the model on unconscious control H_{l}, which is driven by the PML, inevitably includes a large uncertainty.

The modeling accuracy is evaluated by average RMSE. The results of the evaluation are given in Table 1. The large fluctuation in PML control might be caused by psychological effects: the action of the human subject can be affected by various factors

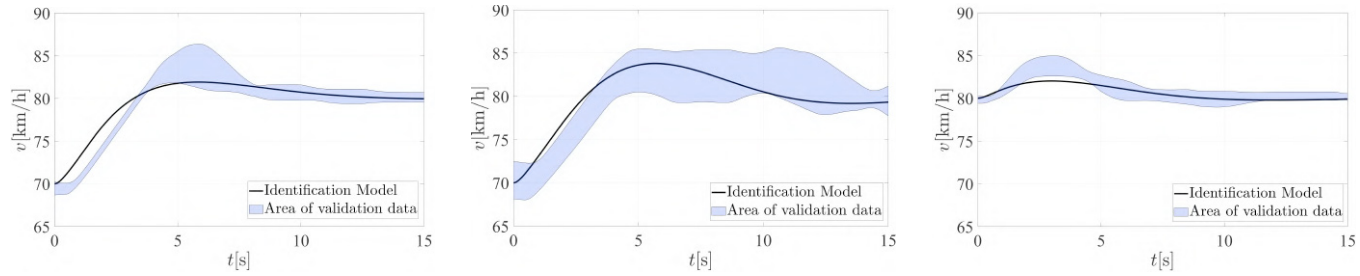

(a) Stage I (b) Stage II (c) Stage III

Fig. 6. Comparisons between validation data and model output,

Table 2. Simulation parameters

constant	magnitude
$(K_i,\ T_i)$	$(4.00,\ 0.25)$
Δt	0.100 s
$k_{\rm s}$	5s
$(\gamma_{\rm on},\ \gamma_{\rm off})$	$(3.00\ {\rm km/h},\ 1.00\ {\rm km/h})$
H	5
$(v_{\min},\ v_{\max})$	$(70.0\ {\rm km/h},\ 90.0\ {\rm km/h})$
$v_{\rm ch}$	$0.100\ {\rm km/h}$
$(q_1, q_2, \cdots, q_H, q_{H+1})$	$(50, 5, \cdots, 5, 20)$
$(r_1, r_2, \cdots, r_H)$	$(30, 1, \cdots, 1)$

such as mood, physical condition, and fatigue, which are not reflected in model $H_{\rm l}$. One can conclude that the constructed model expresses the average behavior of the human subject well. However, some modeling error inevitably exists, in particular for the unconscious control part $H_{\rm l}$.

4.2 Control Simulation

Preparation A numerical simulation was performed, where the presented PML control is applied to a platoon system composed of eleven HDVs, i.e., $N = 10$. We assume that the HDVs have the same dynamics and their models are given by (1) and (8)-(10). The parameters of the HDVs and the PML controller are summarized in Table 2.

The scenario for the control simulation is stated as follows:

- Simulation starts
  At the initial condition, every vehicle including P_0 drives at $80\ {\rm km/h}$ while keeping the distance to the preceding vehicle at $\delta_{{\rm m},i} = 20.6,\ i \in \{1, \cdots, N\}$. At time $k = 0$, HDV 1 enters the tunnel which is located at $z = 0$ and $\delta_{\rm m,1}$ suddenly becomes $5\ {\rm m}$ longer.
- PML starts guiding the drivers
  At time $k = \frac{5}{\Delta t}$, PML is turned on to guide the target drivers that are selected by supervisor $\mathcal{S}$. Then, the state response of the HDVs in the platoon is simulated.

Result of Control Simulation The results of the control simulation with PML are shown in Fig. 7. In these figures, the state behavior of the HDVs labeled by 0, 1, 4, 7, and 10 are shown. The control performance are evaluated using average RMSE, defined by

$$\sum_{i=1}^{N} \frac{1}{N} \sqrt{\frac{1}{n} \sum_{k=\frac{5}{\Delta t}}^{n-1} (v_0(k) - v_i(k))^2},$$

where $n = \frac{30}{\Delta t}$ is the data length, and the minimum velocity of P_{10}. The results of the evaluation are shown in Table 3.

Table 3. State response in platoon without PML control

	Without PML	With PML
Average RMSE	3.78	2.98
min v_{10}	68.7	75.5

We see that the presented PML control significantly improves the performance in two ways: 1) the reduced value in RMSE implies that decelerations of HDVs are compensated; 2) the increase in the minimum value of $v_{10}(k)$ implies that the deceleration propagation from HDV 1 to the following HDVs is mitigated, which contributes to reducing the probability of traffic congestion. Furthermore, we see in Fig. 7(c) that the PML velocity is not frequently changed, which is due to the L_1 norm in the objective function in (6). Infrequent changes in the PML velocity can maintain the driver's trust and improve the reliability of the overall control system.

5. CONCLUSION

In this paper, we addressed light guidance control for a group of human-driven vehicles. First, the model structure of the human driver was presented, where a combination of manual and unconscious control drives the vehicle. Experiments were performed using a driving simulator with VR technology and the collected data was used to estimate the parameters in the presented driver model. Next, the control system design was addressed based on the constructed driver model. Finally, a numerical simulation of PML control was performed, showing the potential of the proposed control system for real-world applications.

Future works include the efficient design of the supervisor aiming at further mitigating traffic congestion, a robust design of the PML control law taking into account the uncertainty in the driver model, and a control simulation that is conducted on a platoon composed of several human subjects in the VR environment.

REFERENCES

Alessandrini, A., Campagna, A., Site, P.D., Filippi, F., and Persia, L. (2015). Automated vehicles and the rethinking of mobility and cities. *Transportation Research Procedia*, 5, 145–160.

Feng, S., Song, Z., Li, Z., Zhang, Y., and Li, L. (2021). Robust platoon control in mixed traffic flow based on tube model predictive control. *IEEE Transactions on Intelligent Vehicles*, 6(4), 711–722.

Hara, K., Inoue, M., and Maestre, J.M. (2021). Data-driven human modeling: Quantifying personal tendency toward laziness. *IEEE Control Systems Letters*, 5(4), 1219–1224.

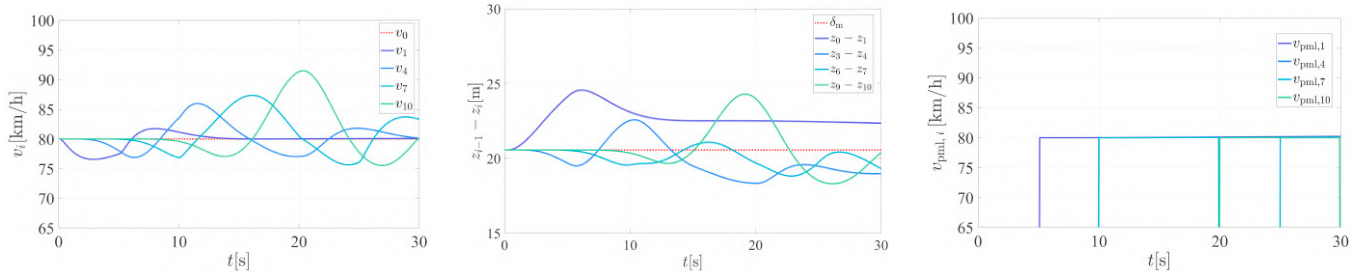

(a) Velocity of HDVs (b) Distance between continuous two HDVs (c) Velocity of PML

Fig. 7. State response in platoon with PML control,

Kari, M., Grosse-Puppendahl, T., Jagaciak, A., Bethge, D., Schutte, R., and Holz, C. (2021). SoundsRide: Affordance-synchronized music mixing for in-car audio augmented reality. In *the 34th Annual ACM Symposium on User Interface Software and Technology*. ACM.

Kawashima, Y., Fukuda, K., and Uchikawa, K. (2012). Determination characteristics for vection yielded by two optical flow. *ITE Technical Report*, 36(52), 17–23.

Koshi, M. and Kuwaham, M. (1992). Capacity of sags and tunnels on japanese motorways. *ITE Journal*, 17–22.

Liu, D., Besselink, B., Baldi, S., Yu, W., and Trentelman, H.L. (2022). On structural and safety properties of head-to-tail string stability in mixed platoons. *IEEE Transactions on Intelligent Transportation Systems*, 1–13.

National Secretariat Technical Research Division (2021). Public call for technology on new road lighting: Results of technical verification. Technical report, Ministry of Land, Infrastructure, Transport and Tourism.

Ozkan, M.F., Rocque, A.J., and Ma, Y. (2021). Inverse reinforcement learning based stochastic driver behavior learning. *IFAC-PapersOnLine*, 54(20), 882–888. Modeling, Estimation and Control Conference MECC 2021.

Rajamani, R. (2011). *Vehicle Dynamics and Control*. Springer Verlag.

Wang, J., Zheng, Y., Xu, Q., Wang, J., and Li, K. (2021). Controllability analysis and optimal control of mixed traffic flow with human-driven and autonomous vehicles. *IEEE Transactions on Intelligent Transportation Systems*, 22(12), 7445–7459.

Watanabe, S., Yanagihara, M., and Oneyama, H. (2018). The effect moving light guide system in traffic jam focued on acceleration behaviors. *Journal of Traffic Engineering*, 4(1), A88–A96.